GNSS Absolute Antenna Calibration at the National Geodetic Survey

Andria Bilich[1] and Gerald Mader[2]
(1) National Geodetic Survey, NOAA, 325 Broadway, Boulder, CO 80305 andria.bilich@noaa.gov
(2) National Geodetic Survey, NOAA, 1315 East-West Highway, Silver Spring, MD 20910

Acknowledgements
Charlie Geoghegan for site setup and calibration operations.
Ernie Marion, Heeyul Han for site operations.

Abstract

The antenna phase center, the point of signal reception for a GNSS antenna, is crucial to precise geodetic applications. It has been well established that phase center patterns differ between antenna models and manufacturers; additional research suggests that the addition of a radome or the choice of antenna mount can significantly alter those *a priori* phase center patterns. As baseline lengths increase, or with antenna mixing, phase center effects on carrier phase data become more pronounced.

We provide the observation models and strategy currently used to generate NGS absolute calibrations, and propose some future refinements. We also show examples of antenna calibrations from the NGS facility. These examples are compared to the NGS relative calibrations as well as absolute calibrations generated by other organizations.

To meet the needs of the high-precision GNSS community, the National Geodetic Survey (NGS) has constructed an absolute antenna calibration facility which uses field measurements and actual GNSS satellite signals to determine antenna phase center patterns. A pan/tilt motor changes the orientation of the antenna under test, and signals are received at a wide range of angles. The phase center patterns will be publicly available and disseminated in both the ANTEX and NGS formats.

1 Facility and Hardware

Calibration Facility

Located in Corbin, Virginia
Two antennas on a short baseline located over a concrete pad (Table 1; Figure 1)
Web camera for site monitoring
South = antenna under test; north = reference antenna

Table 1: site specifications

pad dimensions	8.5 meters x 3.6 meters
pad orientation	short dimension oriented E-W; long dimension oriented N-S
baseline	4.8 meters
current ARP height	0.4918 meters

Pan-tilt Unit (PTU) (Table 2; Figure 2)
Changes the orientation of the antenna under test
Shared point of rotation for both pan and tilt motions
Tribrach adapter, enabling easy mounting of various antennas

Table 2: pan-tilt unit (PTU) specifications

model	Directed Perception Pan-Tilt Unit (PTU-D300)
height dimension	bottom to bracket top = 33.3 cm tilt axis to bracket top = 8.44 cm **tilt axis to ARP = 11.87 cm**
antenna mount	SECO 2070-00 tribrach adapter

Figure 1:
Calibration pad, with reference antenna at the left (north) and test antenna to the right (south).

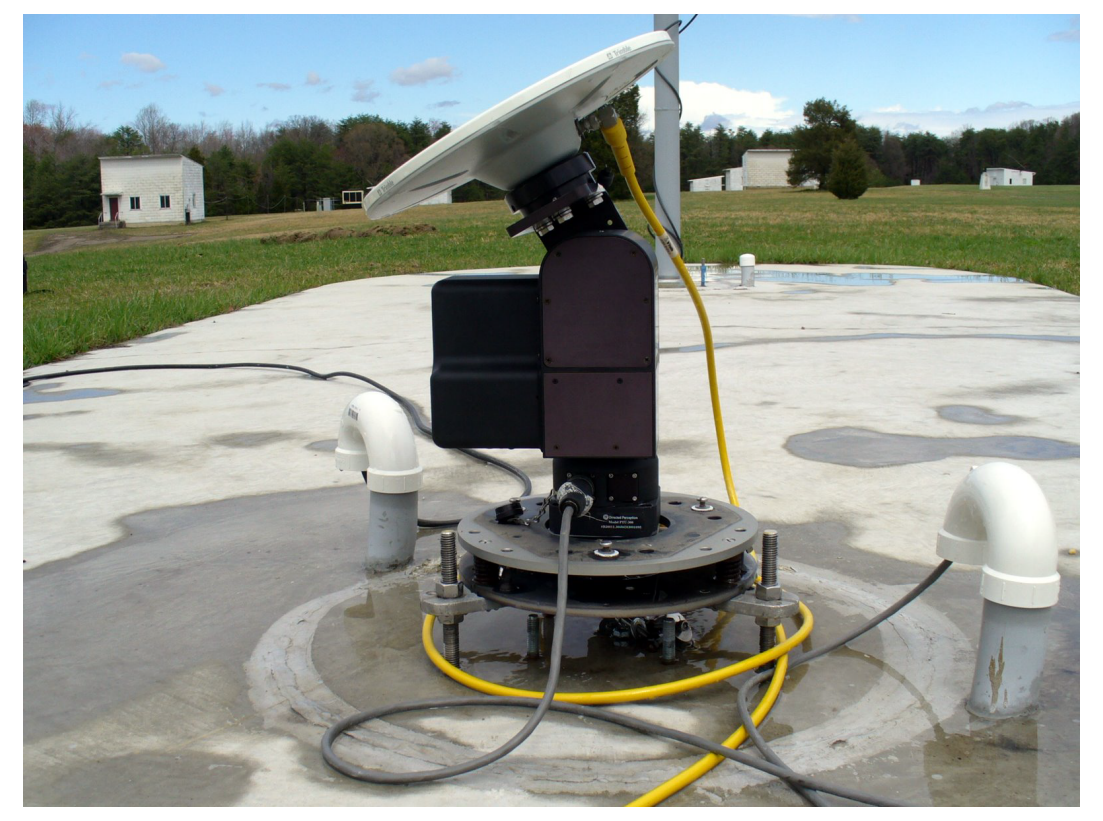

Figure 2:
PTU in tilted position, with Trimble Zephyr Geodetic antenna under test.

Receiver with Common Oscillator

Septentrio PolaRx2eH receiver:
Operating at 1 Hz
Heading receiver = tracks both reference and test antennas with one receiver and uses a common oscillator

Common oscillator:
Unnecessary to double difference to remove the clock, or to estimate a differential clock
Still exhibits a hardware bias between two antennas observed.
Hardware bias is time-variable but slowly varying (Figure 3) = can be considered constant over a time interval of 20 seconds (possibly more).

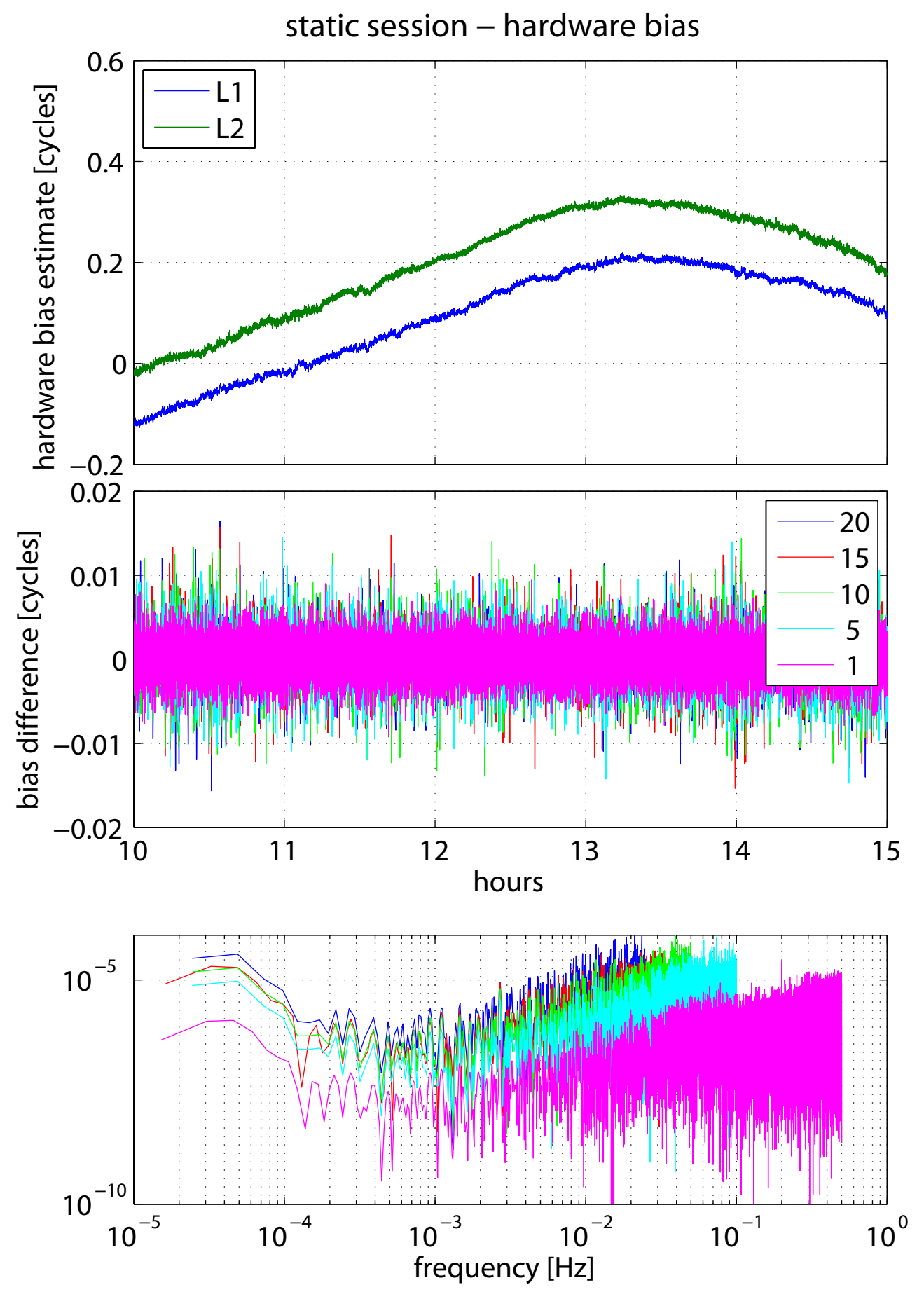

Figure 3:
Behavior of hardware bias during 5-hour static observation session.
Top: estimated biases on both GPS frequencies
Center: time difference of bias for different time intervals, 1 to 20 seconds.
Bottom: power spectra of hardwre time differencs; behavior is largely white noise.

2 Data and Process

A Motion Scenario

Pan-tilt unit (PTU) motion:
Moves through large range of pan and tilt values to cover the entire range of positive elevation angles (Figure 5).
Full coverage not possible with stationary antenna (Figure 4)
Tilts = limited to between -60 to +30 deg to maintain tracking
Pans (rotations) = -180 to +180 deg
At each pan, antenna moves between 0 tilt and several non-zero tilt values (see Section B)
Full motion scenario takes ~ 4 hours
Conduct the same motion scenario twice, once with the antenna oriented north (Figure 5a) and once oriented east (Figure 5b), to obtain better sky coverage

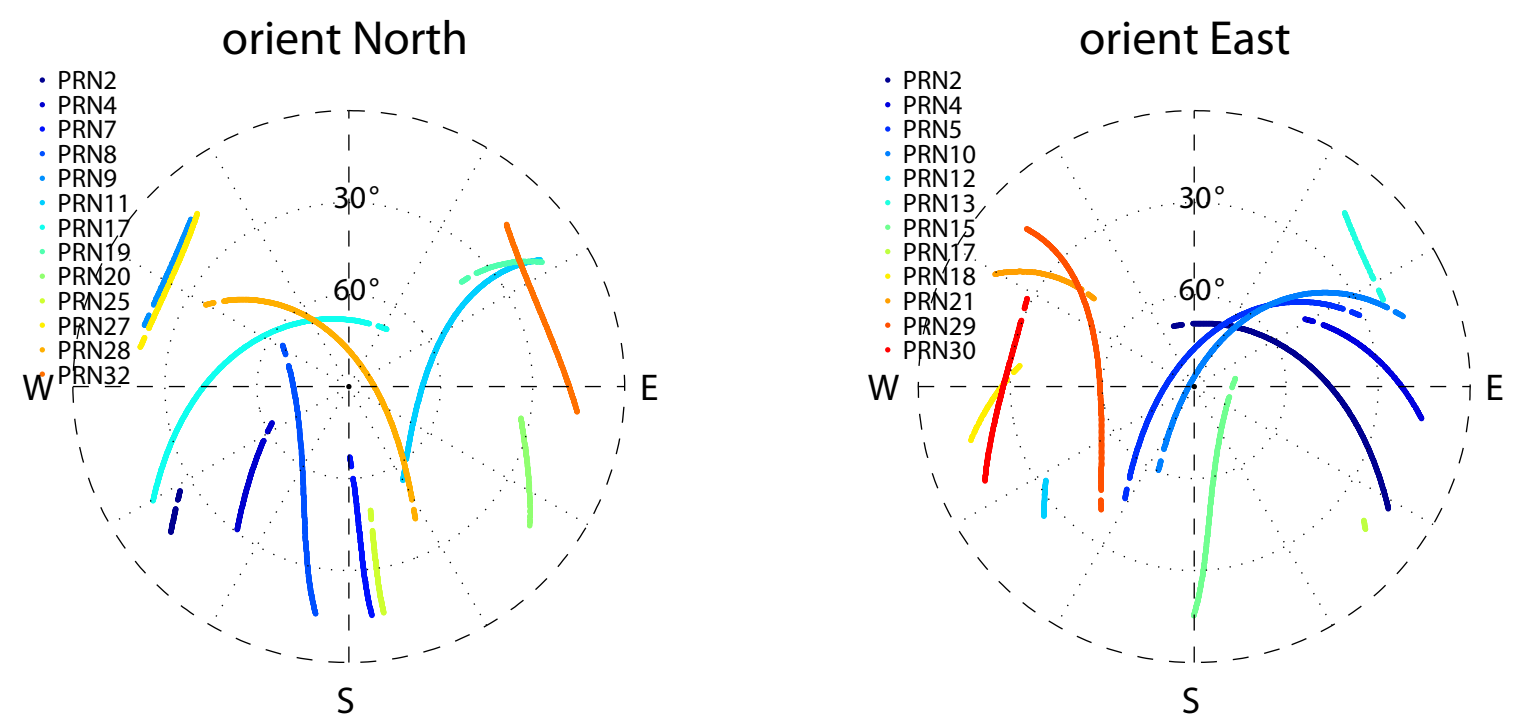

Figure 4:
Satellites in view over 4 hours, given in local reference frame. Two different sessions are shown, corresponding to the North and East orientations of the test antenna on the PTU (Figure 5). A 15 deg elevation angle cutoff was imposed.

Figure 5:
Points of reception in the test antenna body frame, for north (top) and east (bottom) orientations of the test antenna on the PTU. Colors depict the number of points observed in a 1 x 1 Cartesian grid; most grid squares contain 6 or more data points. Both the upper (left) and lower (right) hemispheres of the test antenna are shown.

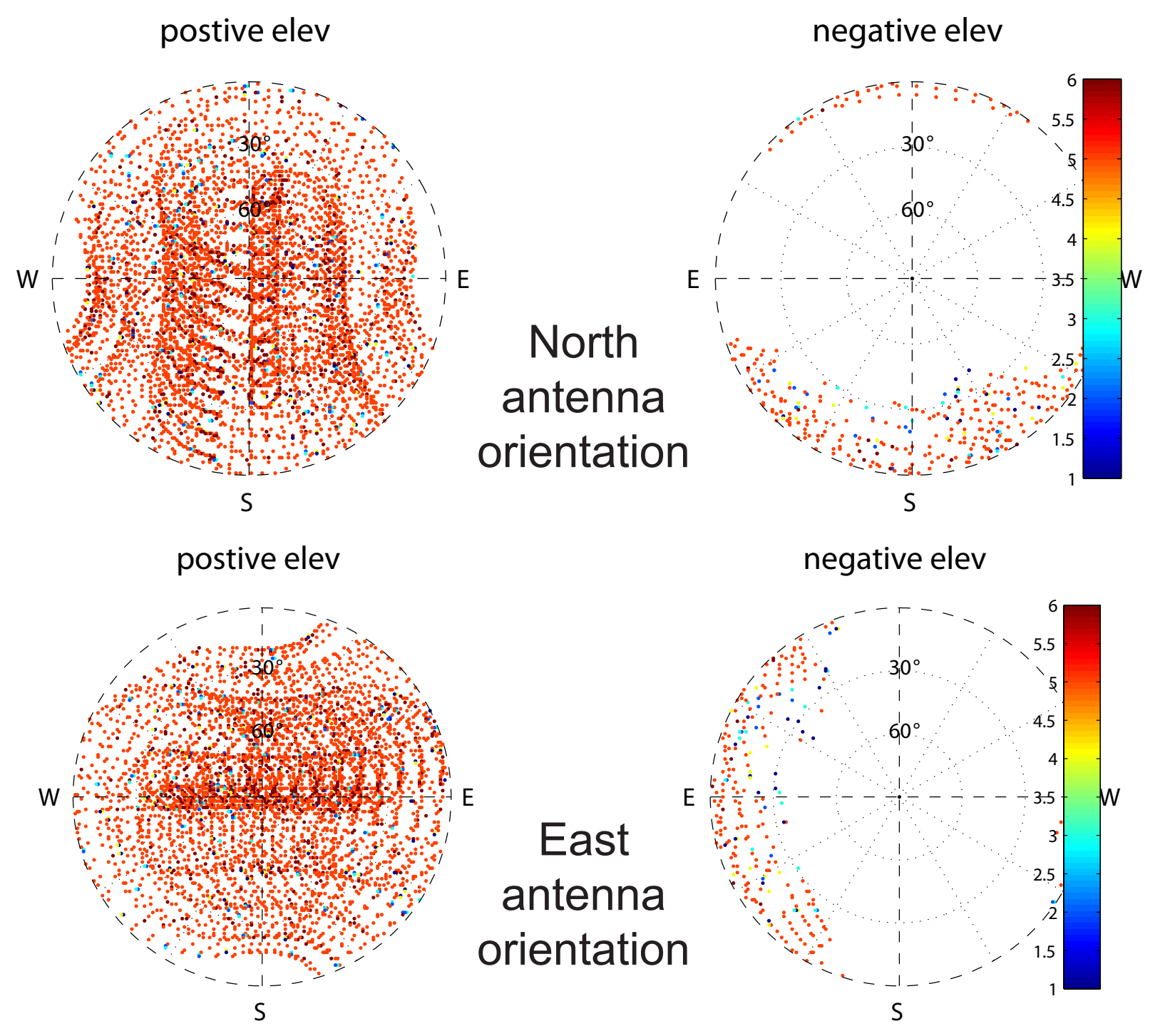

B Single Difference (SD): Accounting for Antenna Motion

Interstation single differences (SD):
Formed for each satellite
Removes both satellite and receiver clock effects
Short baseline (4.8 m) = removes tropospheric and ionospheric delays
SD edited to remove cycle slips and integer ambiguities

$$\delta\phi_{test} = clk + \delta_{test} + T + I + PCV_{test} + MP_{test}$$
$$\delta\phi_{ref} = clk + \delta_{ref} + T + I + PCV_{ref} + MP_{ref}$$

$$\begin{aligned} SD &= \delta\phi_{test} - \delta\phi_{ref} \\ &= \Delta\delta_{ref} + \left(PCV_{test} - PCV_{ref}\right) + \left(MP_{test} - MP_{ref}\right) \end{aligned}$$

Known effects modeled and removed (Figure 6):
PTU rotation arm – 11.87 cm from rotation point to antenna ARP
a priori phase center - determined via solution with 4 hours of static data
Phase windup - apply correction of Wu et. al (1993), accounting for antenna tilts as well as antenna rotations

Figure 6:
Top: after editing, the edited single difference phase (SD) are dominated by geometric effects, i.e. the projection of the PTU rotation arm + a priori phase center onto the satellite line of sight.
Bottom: after removing geometric effects (SDP-PTUarm-NEU), single difference phase are affected by phase windup, which is removed to yield final edited SD.

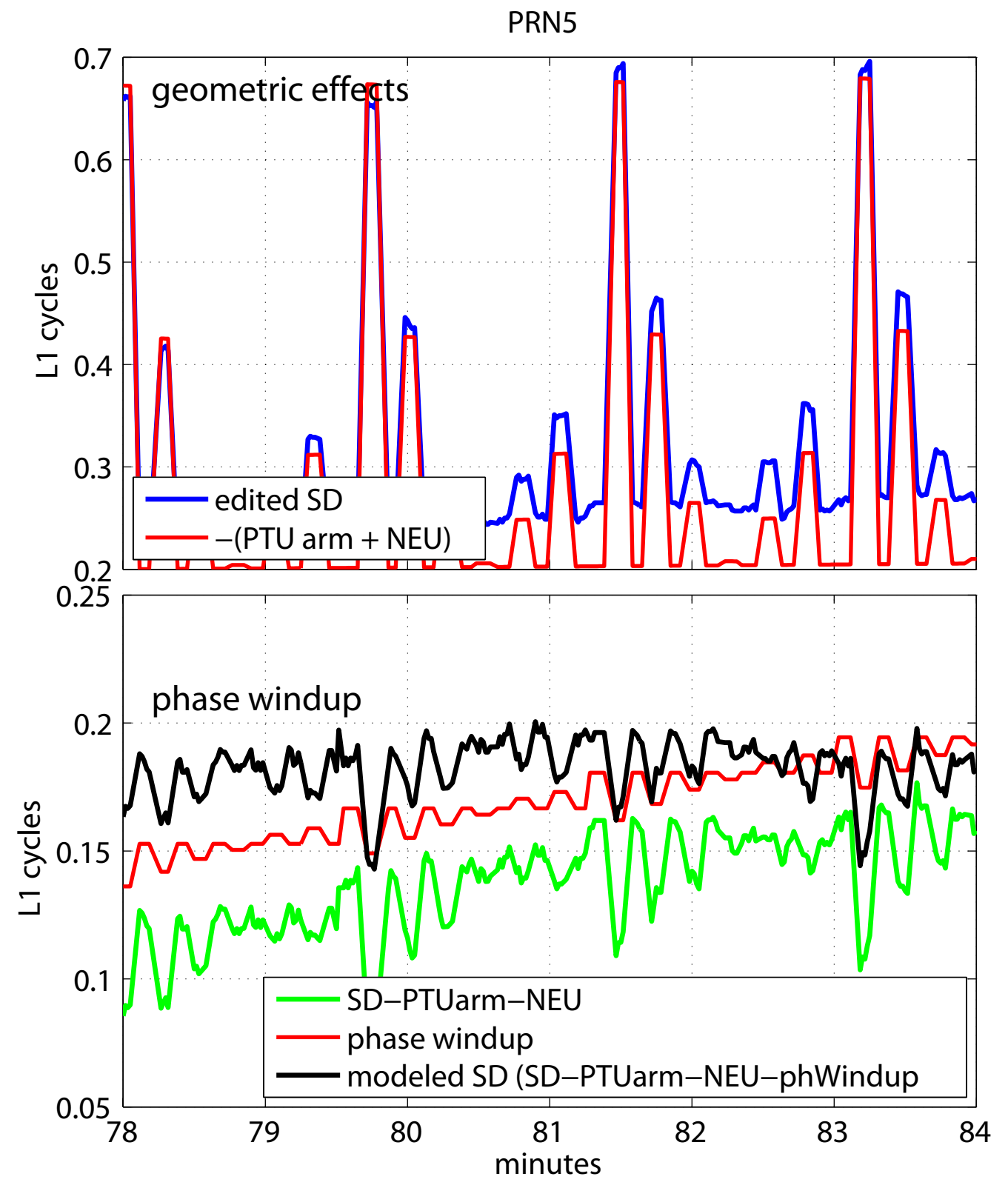

The final edited SD data (Figure 7) show a **clear dependence on angular changes created by pan/tilt motions**, with small variations of a few 1/100's of a cycle ... largely due to antenna phase center variations.

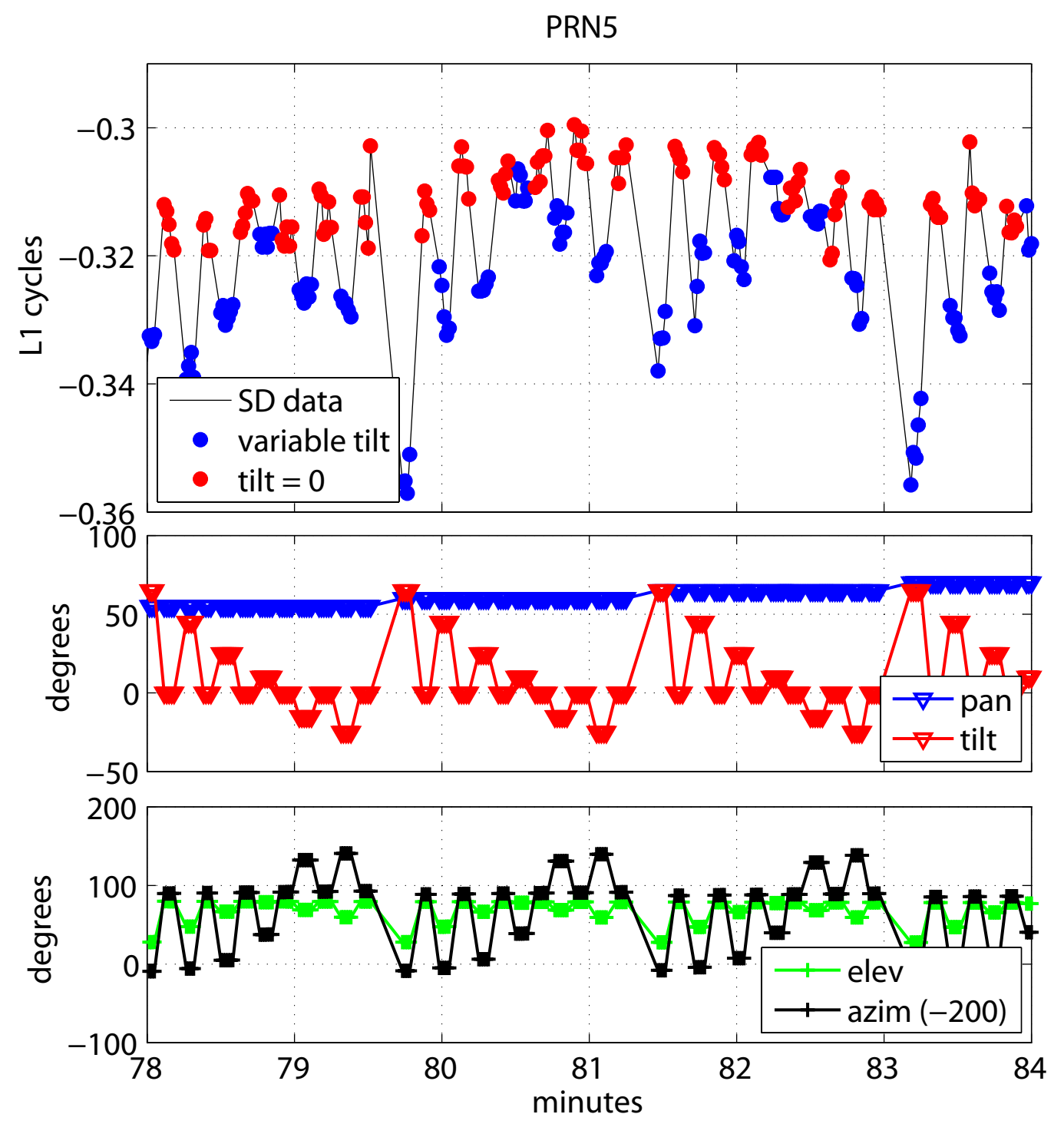

Figure 7:
L1 edited SD for PRN5 (top), plotted alongside the associated PTU motions (center) and observed satellite elevation and azimuth angle (bottom) in the antenna body frame.

C Time Difference of Single Difference (TDSD): Removal of Reference Antenna Effects

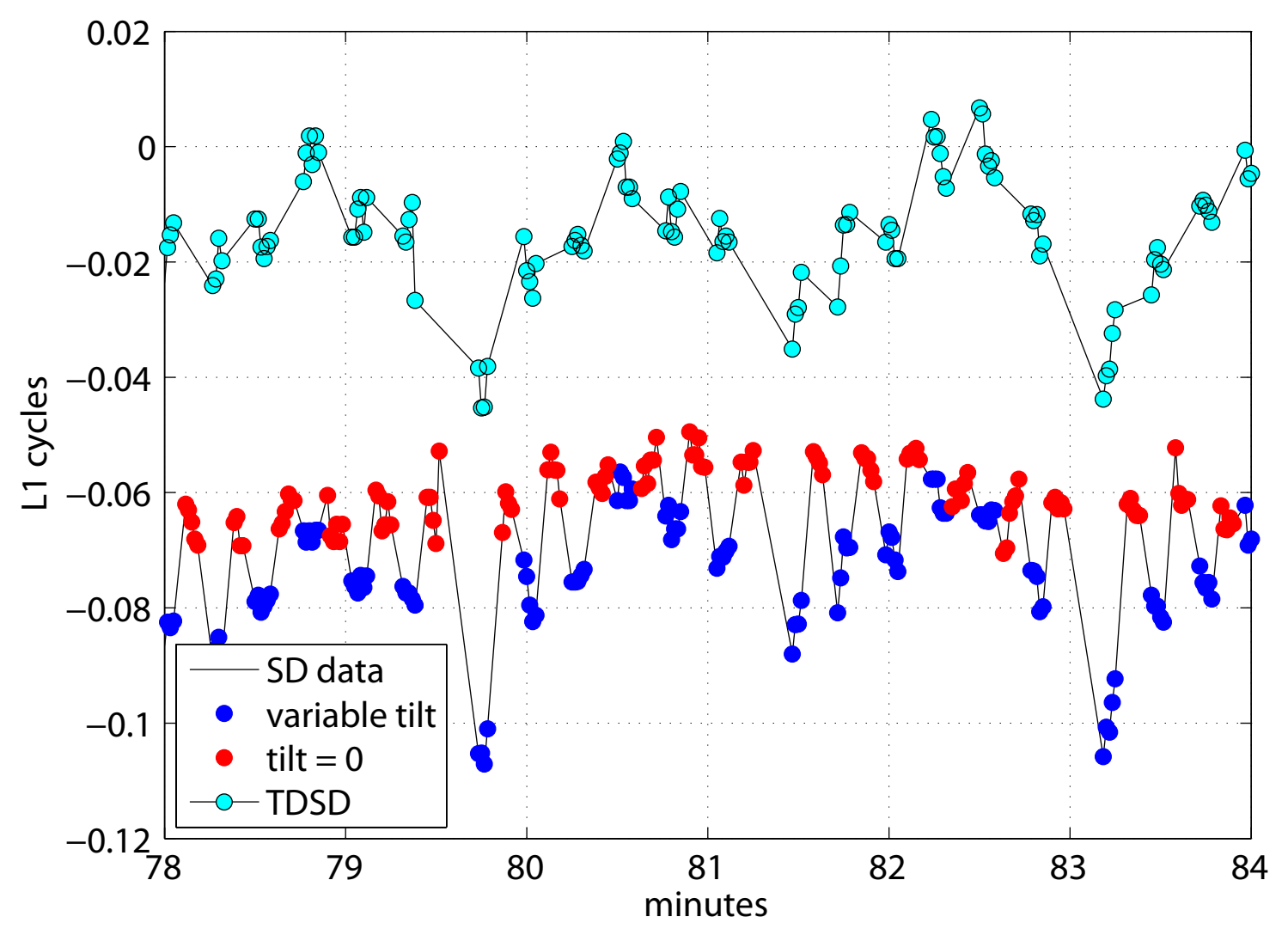

Figure 8:
L1 edited single difference (SD) for PRN5, repeated from Figure 7, now plotted alongside the time difference single difference (TDSD) formed from the SD tilted vs. untilted pairs. TDSD data are used to solve for the phase center pattern.

TDSD independence from choice of reference antenna:
Example calibrations for same test antenna, but using different reference antennas
Geo++ L1 absolute calibration values for reference antennas [chokering (ASH700936D_M); Zephyr Geodetic] differ by up to a centimeter (Figure 10)
TDSD data and the elevation angle dependent calibrations are nearly identical (Figures 10, 11)

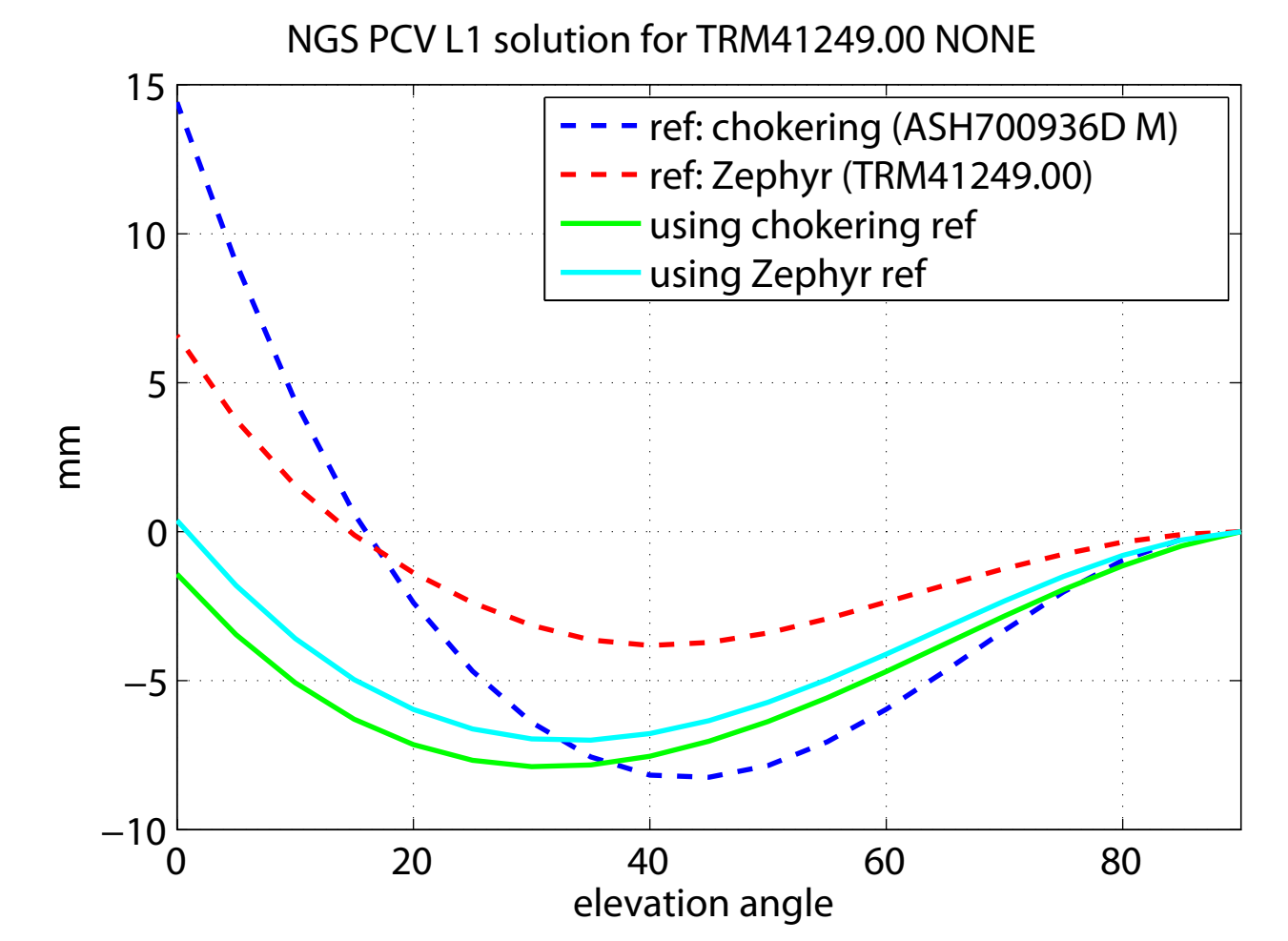

Figure 10:
Comparison of L1 PCV patterns of reference antennas (dashed lines), plotted against the resulting NGS absolute calibrations (solid lines) determined using these very distinct reference antennas.

Absolute calibration = independent of the reference antenna:
Single difference data still contain two reference antenna effects – phase center variations and multipath
Time differences of the single differences (TDSD) remove both effects

$$\begin{aligned} TDSD_{ij} &\equiv SD_i - SD_j \\ &= \Delta\delta_i + PCV_{test}(\theta_i,\alpha_i) - PCV_{ref}(\theta^{ENV},\alpha^{ENV}) + \left(MP_{test_i} - MP_{ref}\right) \\ &\quad -\left[\Delta\delta_j + PCV_{test}(\theta_j,\alpha_j) - PCV_{ref}(\theta^{ENV},\alpha^{ENV}) + \left(MP_{test_j} - MP_{ref}\right)\right] \\ &= PCV_{test}(\theta_i,\alpha_i) - PCV_{test}(\theta_j,\alpha_j) + \Delta MP_{test_{ij}} \end{aligned}$$

TDSD pairs (Figure 8):
Closely spaced epochs = satellite has not moved significantly (Figure 9) = PCV and multipath at the reference antenna is unchanged
Pairs with zero tilt vs. nonzero tilt (Figure 7) = create large contrast between the reception angles in the antenna body frame

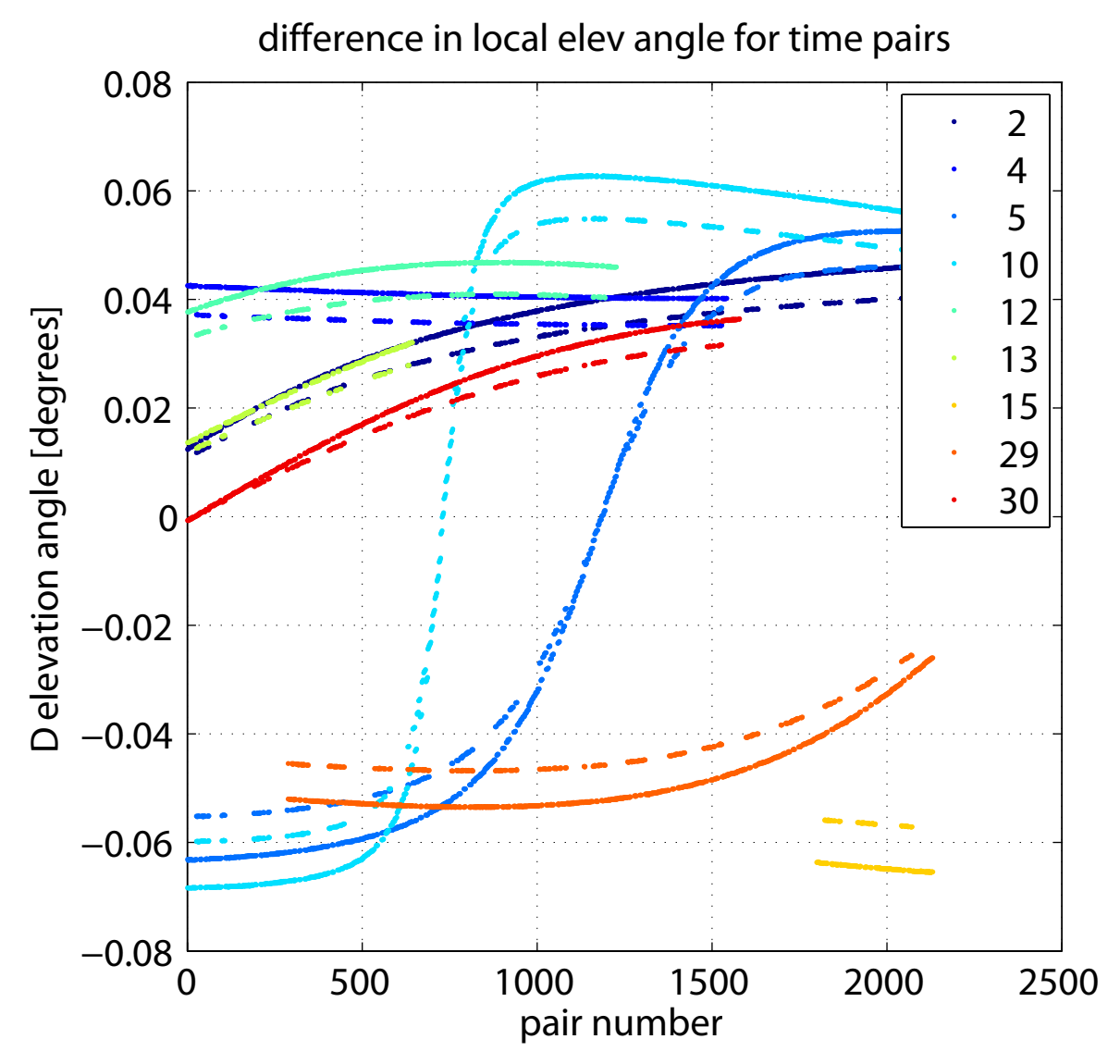

Figure 9:
Change in elevation angle observed by the stationary reference antenna for time difference pairs, given for individual satellites in view. The dashed appearance results from a variable time separation of 7 or 8 seconds used with this data set.

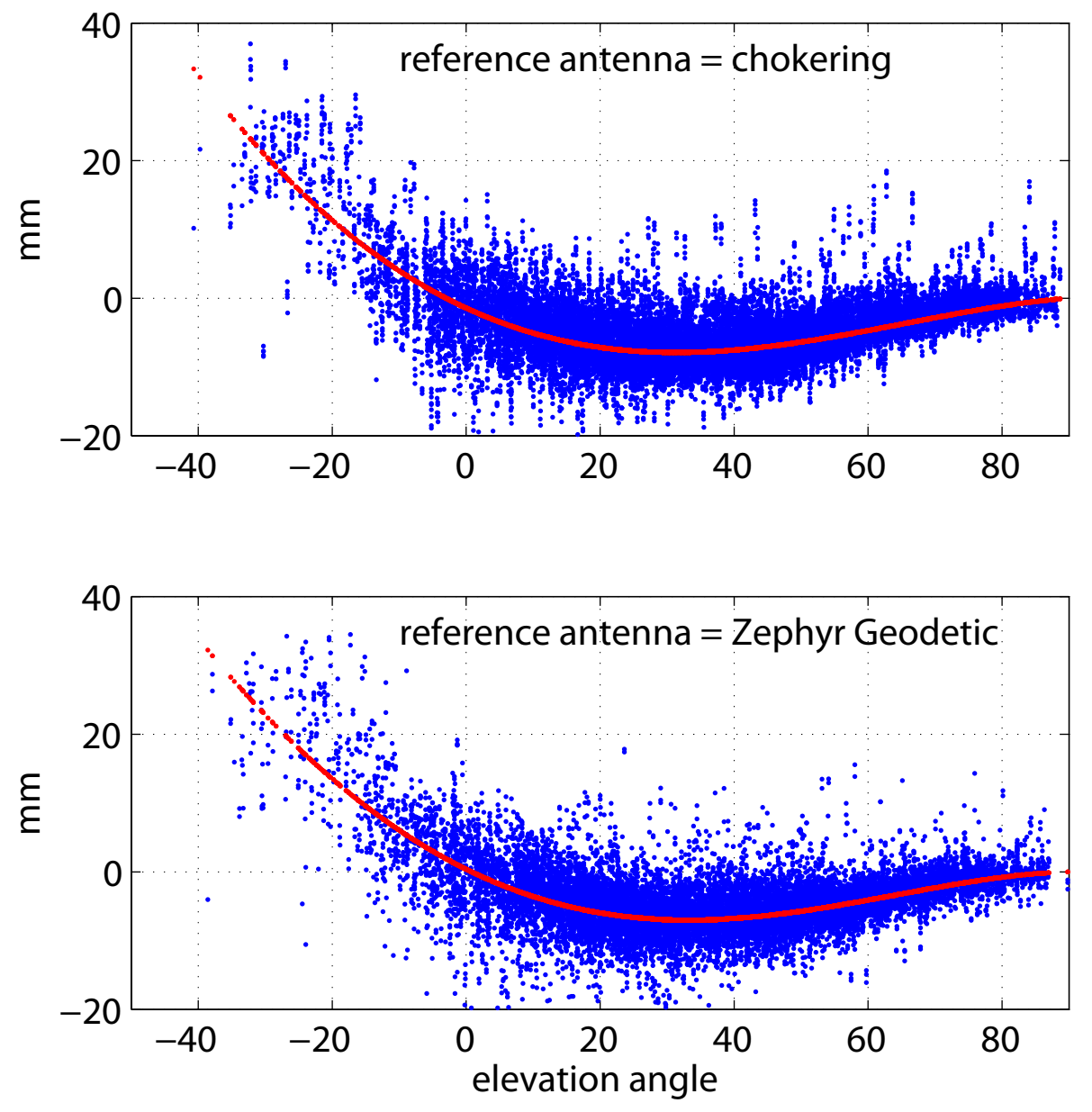

Figure 11:
TDSD data plotted as a function of elevation angle in the antenna body frame. The red line shows the PCV solution using these data.

3 Calibration Results

Early calibration results show great promise. Both a priori phase center values (Table 3) and elevation-dependent phase center variation (PCV) patterns (Figures 12-13) are consistent with Geo++ absolute calibration values, but differ by a few millimeters. The discrepancy between NGS and Geo++ calibrations is within the noise boundaries of TDSD data, meriting further research into TDSD noise minimization.

Calibrations shown here are shown only for a 3rd order polynomial fit as a function of elevation angle (in the antenna frame). Future work includes determining phase center dependence on azimuth angle to provide a 3-D picture of PCV.

Trimble Zephyr Geodetic
with groundplane (TRM41249.00)

Ashtech Geodetic III "Whopper"
with groundplane (ASH700718B)

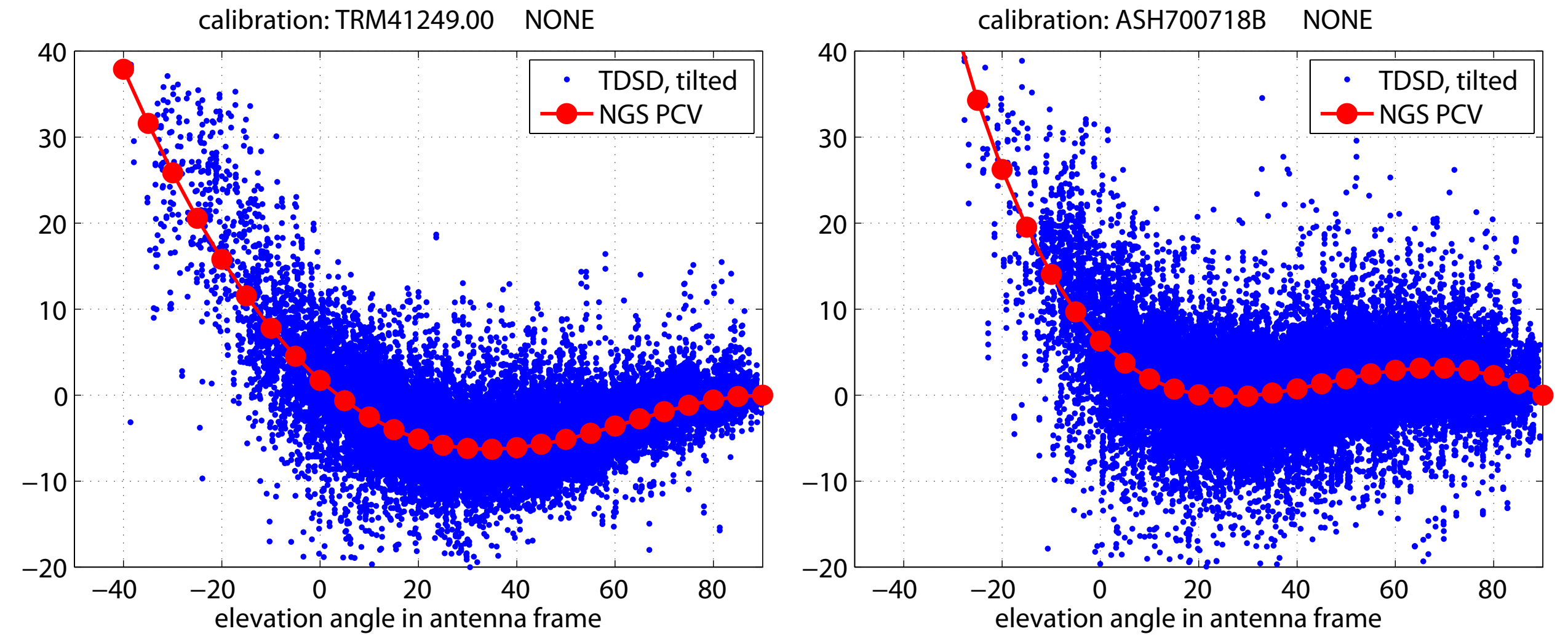

Figure 12:
TDSD data versus 3rd order polynomial fit. Polynomial fit is determined via least squares and is a function of elevation angle in the antenna frame.

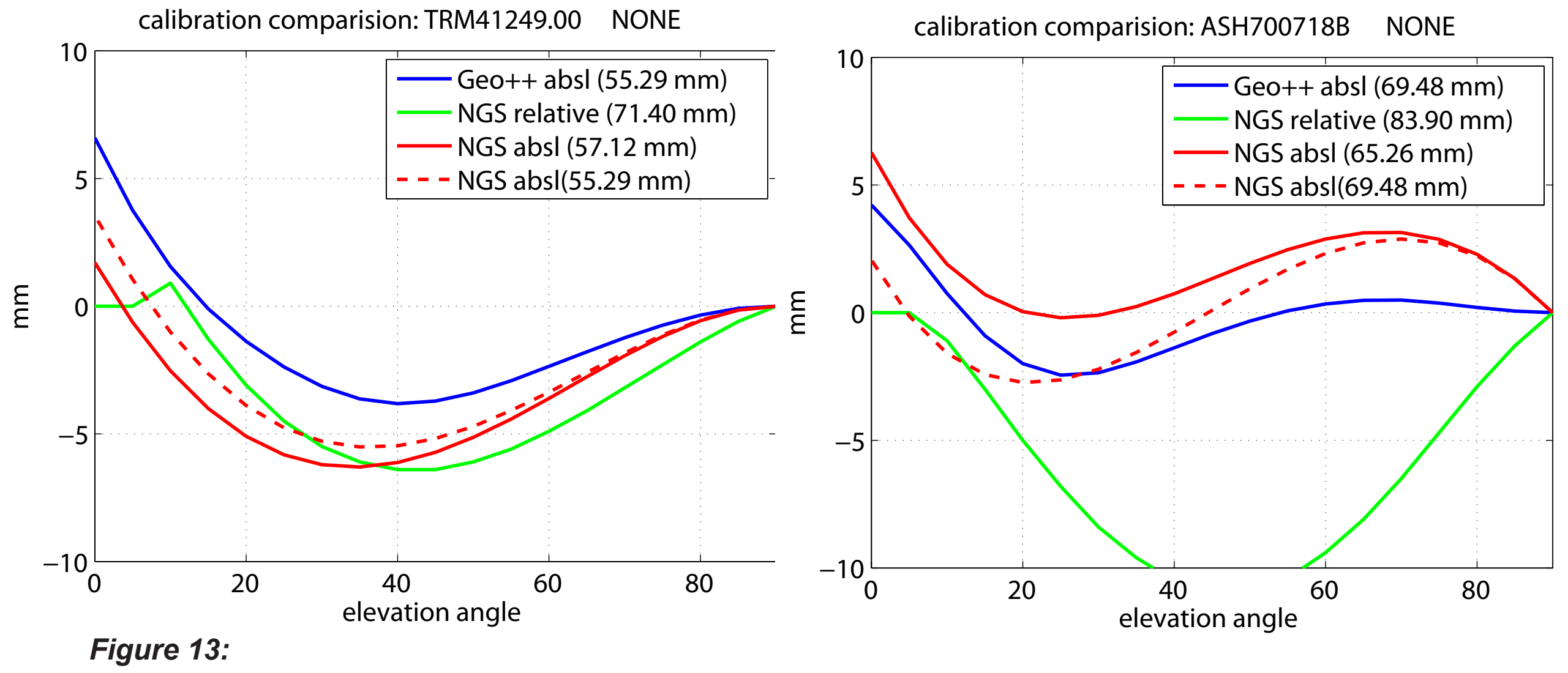

Figure 13:
Comparison of Geo++ absolute calibration PCV values to the NGS solution shown here. The dashed red line gives the translated NGS PCV pattern if the NGS a priori phase center were made equivalent to the Geo++ a priori value. NGS relative calibrations are shown for historical value.

	N	E	U	(mm)
Geo++	-0.08	0.55	55.29	
NGS rel	0.30	0.50	71.40	
NGS absl	-0.10	-1.79	57.12	

	N	E	U	(mm)
Geo++	-1.67	-0.47	69.48	
NGS rel	-0.60	0.20	83.90	
NGS absl	1.37	-2.98	65.26	

Table 3:
A priori phase center values for Geo++ absolute calibration, NGS relative calibration, and new NGS absolute calibration, given in mm relative to the antenna ARP.

4 Future Work

Azimuthal dependence of PCV – determine optimal method (spherical harmonics, surface fit, other?)
Noise reduction
  Account for or change receiver dynamics – L2 tracking highly sensitive to acceleration
  Time separation of data
  Reassess orbit calculations and travel time assumptions
Multipath
  Proper choice of PTU height above the ground
  Quantify effects of antenna height changes when antenna undergoes tilt
Resurvey for a priori monument locations, rotation of PTU relative to local east/north/up reference frame
Assess repeatability of PCV estimates and dependence on PTU dwell time.
Upgrade PTU equipment for 3rd axis of rotation, or automate 90 antenna rotation